Materials Research
Express



PAPER

# Enhancement of photocatalytic efficiency using heterostructured $SiO_2$–$Ta_2O_5$ thin films

To cite this article: Arabinda Baruah *et al* 2015 *Mater. Res. Express* **2** 056404



Materials Research Express

RECEIVED
15 January 2015

REVISED
25 March 2015

ACCEPTED FOR PUBLICATION
27 April 2015

PUBLISHED
27 May 2015

PAPER

# Enhancement of photocatalytic efficiency using heterostructured $SiO_2$–$Ta_2O_5$ thin films

**Arabinda Baruah**[1], **Menaka Jha**[1], **Santosh Kumar**[2] **and Ashok Kumar Ganguli**[1,2]

[1] Department of Chemistry, Indian Institute of Technology, Delhi, HauzKhas,New Delhi-110016, India
[2] Department of Chemistry, National Institute of Technology, Warangal-506004, A.P., India
[3] Institute of Nano Science and Technology, Habitat Centre, Phase-X, Sector—64,Mohali, Punjab—160062, India

**E-mail:** arabind24@gmail.com **and** ashok@chemistry.iitd.ernet.in

**Keywords:** tantalum pentoxide, silica, Langmuir–Blodgett film, thin films

Supplementary material for this article is available online

## Abstract

Fabrication of controlled layered structured thin films with tunable physical properties is an important area of research as thin film technology holds potential for a variety of industrial applications. In the present work, we have demonstrated the process for fabrication of multilayer films of silica and tantalum oxide by Langmuir–Blodgett film fabrication technique and investigated their photocatalytic degradation efficiency for organic dye (Rhodamine B) under UV radiation. The photocatalytic degradation of RhB in presence of $SiO_2$–$Ta_2O_5$ exhibited remarkably enhanced photocatalytic activity than pure $Ta_2O_5$. This is because of the high separation efficiency of photo-generated electron–hole pair due to the Lewis acidity of silica and the greater contact area between these two layers. The $SiO_2$–$Ta_2O_5$ system was optimized for the number of self-assembled layers of silica and tantalum oxide, and it has been found that 10S–15T–10S–15T–10S–15T (where S and T represents $SiO_2$ and $Ta_2O_5$ respectively) pattern has been found to have maximum photocatalytic degradation efficiency of 71% (with 18% degradation per unit area of the film) which is 3.5 fold higher than pure $Ta_2O_5$ under identical experimental condition. Also, the photocatalytic activity of these films was also proved to be sensitive to the sequence of silica and tantalum oxide layers when the film area of all the samples was kept constant (3.75 $cm^2$). Further analysis confirms that the degradation of dye molecules has been largely promoted by the photo generated holes, rather than the super oxide radical anions.

## 1. Introduction

Semiconductor metal oxides (in bulk as well as in thin film form) have attracted attention due to their fascinating optical and electronic properties which have applications in photocatalysis [1], photovoltaics [2], microelectronics [3] and thermoelectrics [4]. Each of these applications requires a thorough understanding of the materials chemistry of these oxides in bulk, nano and in thin film form. In metal oxide thin films, the properties are also dependent on the interaction of metal oxide with substrate and thickness of the film [5]. Much of the research in this area is emphasizing the control of layer thickness of films. A number of semiconductor materials have been reported in literature for photocatalytic degradation of dye molecules in water. Among them, $TiO_2$, ZnS, CdS, ZnO, $Fe_2O_3$ and their composites have been explored in both powder as well as in thin film form for various photo-induced redox reactions [6–10]. However, to the best of our knowledge there are very few reports on photocatalytic studies of tantalum oxide and its composites [11–13]. $Ta_2O_5$ is a wide band gap photocatalyst (4.1 eV) with tuneable band positions and thus a suitable candidate for various light-induced redox reactions [13]. Also, it is known that the photocatalytic efficiency of the semiconductor material depends on several factors, like, surface area, particle size, crystallinity, surface defects, electronic band structure etc [14]. Large surface area is also beneficial for adsorption of organic pollutants, which further enhances efficiency of the photocatalyst, since the adsorption of pollutants is the initial step of the

photocatalytic degradation [15]. Silica has been used as a support material in many of the composite photocatalysts due to its high surface area, easy availability and low cost [16]. Also, metal oxide thin films have been fabricated by physical route (electroplating, evaporation, molecular beam epitaxy, pulsed laser deposition and plasma enhanced chemical vapour deposition) which requires complicated and expensive equipments [17]. Though there are several chemical routes for fabrication of oxide thin films (spin coating, dip coating, spray coating, sol–gel method and atomic layer deposition) however, the control of layer thickness to get monolayer coverage is still a challenging task [18, 19]. To make thin films with controlled layer thickness, Langmuir–Blodgett (LB) film deposition technique provides a convenient way of depositing self-assembled mono-molecular layers of amphiphilic molecules on various substrates. So far, only few reports on LB films of $TiO_2$, $SiO_2$, CdS, CuO and ZnO are available in literature, where these films were explored for photocatalytic applications [20–22]. To the best of our knowledge, there has been no report so far on LB films fabrication process for tantalum oxide. The major advantage of using this technique for the preparation of thin films is that highly uniform solid films of controlled thickness can be deposited over a large surface.

Thus, the motivation behind the present work is to make $SiO_2$–$Ta_2O_5$ thin films with controlled layer structure (like thickness and order of deposition of silica and tantalum pentoxide) using LB technique and study their photocatalytic properties. The thickness and the pattern of alternately deposited layers of silica and tantalum oxide have been controlled in order to improve the photocatalytic efficiency of the films. We have also synthesized $SiO_2$–$Ta_2O_5$ composites and compared their photocatalytic efficiency with the multilayered thin films. The photocatalytic degradation efficiency of these heterostructured thin films is found to be higher than their bulk counter parts (composites) and much higher than bare $Ta_2O_5$. This enhancement can be attributed to the higher adsorption capacity of the silica layers owing to their higher surface area and Lewis acidity, which helps in delaying the recombination of photo-generated electron hole pairs. LB deposition technique facilitates maximum area of contact between the thin layers of silica and tantalum oxide, which is also crucial for electron transport and band gap modification.

## 2. Experimental

### 2.1. Materials

All the chemicals used were of analytical grade and were used without any further purification., phenyltriethoxysilane (Ph-TEOS, Sigma Aldrich), Tantalum isopropoxide (Alfa Aesar),chloroform (Fisher Scientific), Cetyltrimethyl ammonium bromide (CTAB) (Spectrochem Laboratories), liquor ammonia (Rankem), absolute ethanol (Merck), ethanol (Merck) and ammonia solution (Fisher scientific) were used as obtained. For the preparation of LB films, quartz substrates were used. The substrates were thoroughly cleaned prior to use. They were immersed in a 1:1 mixture of chromic acid and sulphuric acid for 30 min, rinsed with distilled water and finally dried at room temperature.

### 2.2. Synthesis of silica and tantalum pentoxide and fabrication of their thin films

In order to obtain LB films of silica nanoparticles, initially, phenyl functionalized silica particles were prepared by Stöber's process [23]. In brief, 0.17 M Ph-TEOS was added to the mixture of 2.0 M ammonia and 6.0 M $H_2O$ in ethanol. After stirring for 24 h, the suspension was centrifuged at 3000 rpm for 30 min. For the synthesis of tantalum pentoxide ($Ta_2O_5$), tantalum isopropoxide [$Ta(O^iPr)_5$] was hydrolyzed by aq. ammonia. Further, the as obtained phenyl-silica or $Ta_2O_5$ particles were washed with ethanol and then re-dispersed in chloroform (0.01 mg $mL^{-1}$).

For the preparation of LB films, we used the Apex Instruments LB Film Deposition unit. The Teflon trough was filled with Millipore water, and the water surface was cleaned five times before spreading the sample solutions. Further, 500 $\mu$L of the chloroform solution containing the phenyl silica was spread carefully over the water sub-phase in the Teflon trough for LB film deposition. A strip of Whatman filter paper was used as the sensor plate in Wilhelmy film balance. 20 mm length of quartz substrate was immersed into the water prior to the spreading of the particles. By slowly decreasing the available area (at the rate of 5 mm per minute) for molecules at the air–water interface, a continuous Langmuir film was formed. For the deposition of $Ta_2O_5$ films, a solution of tantalum isopropoxide in chloroform (0.01 mg $mL^{-1}$) was used. After being dispensed over the water sub-phase, chloroform gradually evaporated from the air–water interface and tantalum isopropoxide got hydrolyzed as soon as it came into contact with water. Barrier compression was initiated after 20 min of dispensing the sample. Thin films having multilayered structures with varying number of layers of silica and tantalum oxide were fabricated using LB film technique as shown in table S1.

After film deposition, the films were heated at 650 °C for 6 h in air, so that the phenyl groups got removed and we were left with pure silica and tantalum oxide multilayered films. The photocatalytic studies of these films have been carried out.

### 2.3. Synthesis of silica–tantalum oxide composite

The $SiO_2$–$Ta_2O_5$ composite powder was synthesized by the hydrolysis of tantalum isopropoxide and TEOS using hydrothermal method. 0.50 g of CTAB and 0.25 mL (1 mole) of TEOS were dissolved in mixture of 7 mL of water and 6.3 mL of ethanol solution. The reaction mixture was stirred for 30 min at room temperature and then 0.25 mL of tantalum isopropoxide was added followed by 0.5 mL of 25% ammonia solution drop wise. The resulting mixture was then loaded in a Teflon vessel kept in a hydrothermal bomb and heated at 120 °C for 48 h. The contents were centrifuged, washed with water followed by ethanol, and dried at 70 °C and further heated at 650 °C for 6 h in air.

### 2.4. Photocatalytic studies

The photocatalytic activity of the films was evaluated by the degradation of Rhodamine B dye under UV irradiation. The photocatalytic reactions were carried out in a quartz reactor with a water circulating jacket. Experiments were also performed in the absence of photocatalyst and illumination (blank tests). For the photocatalytic degradation of Rhodamine B, films containing different amounts of catalyst were introduced into the beaker containing 20 mL of 10 $\mu$M Rhodamine B (pH = ~8.9). In order to ensure the adsorption/desorption equilibrium between the dye molecules and the catalyst films, stirring was kept on for 30 min without illumination. Then the UV lamp (125 W high pressure Hg lamp) was mounted above the reactor and switched on. After every 10 min, one mL of dye solution was taken out and the absorbance of the organic dye in solution was measured at 553 nm as a function of the irradiation time using a UV–vis spectrophotometer (Shimadzu UV-2450) and then it was put back. The degradation efficiency of a photocatalyst can be defined as follows:

$$\text{Degradation}\,(\%) = (1 - C/C_o) \times 100\%,$$

where, $C_o$ is the concentration of Rhodamine B dye at the adsorption equilibrium and $C$ is the residual concentration of the dye at different illumination intervals.

## 3. Characterization

The x-ray diffraction patterns of the LB films were recorded using XPERT-PRO Glancing Angle x-ray Diffractometer by scanning at $2\theta$ values ranging from 0.5° to 50°. Surface morphology and the film thickness have been studied using an atomic force microscope (Nanoscope VEEGA). Size and morphology of the hydrolyzed molecules were observed using FEI Technai $G^2$ 20 transmission electron microscope operating at 200 kV. Samples were prepared on carbon coated copper grids by deposition of the self-assembled monolayers on the grid. Powder x-ray diffraction for the ph-$SiO_2$ and $Ta_2O_5$ composite powder was also recorded with a Bruker D8 Advance Diffractometer using Ni-filtered Cu-K$\alpha$ radiation (10°–70° in $2\theta$). To visualize the multi-layered structure of the films, the field emission scanning electron microscopy (FESEM) studies were carried out using FEI Quanta 3D FEG/FESEM at an accelerating voltage of 20 kV. For recording the diffuse reflectance spectra of the samples, UV–Visible spectrophotometer (Shimadzu UV-2450), was used in the wavelength range of 200–800 nm with barium sulphate as the reference. The resulting reflectance information was converted into band-gap by using Kubelka–Munk equation. Nitrogen gas adsorption–desorption isotherms were recorded at liquid nitrogen temperature (77 K) using a Nova 2000e (Quantachrome Corp.) equipment and the specific surface area was determined by the Brunauer–Emmett–Teller (BET) method for the silica particles. The amount of deposited photocatalyst material on the quartz substrate was estimated from the difference in the weight of the film coated substrate and the bare substrate. Here, it has been assumed that the geometrical surface area of the top surface of the photocatalyst films on the quartz substrates, which actually comes into contact with the dye solution, remains constant. The film area (3.75 $cm^2$) has been obtained by multiplying the length (2.5 cm) and the breadth (1.5 cm) of the deposited film.

## 4. Results and discussion

In order to prepare LB films of silica nanoparticles, initially, phenyl functionalized silica nanoparticles were prepared by Stöber's process. Spherical nanoparticles having size 70–80 nm (figure S1) were obtained by alkaline hydrolysis of ph-TEOS.

### 4.1. Control of film properties of silica and tantalum pentoxide

Figures 1(a) and (b) show the isotherms for the LB film deposition of phenyl-silica and $Ta_2O_5$ respectively. From the shape of the surface pressure versus area isotherm curves, the proximity among molecules floating at the air–water interface and their orientation can be understood. The isotherm for phenyl-silica (figure 1(a)) can be divided into three segments. The first segment shows a gradual increase in surface pressure as the available area

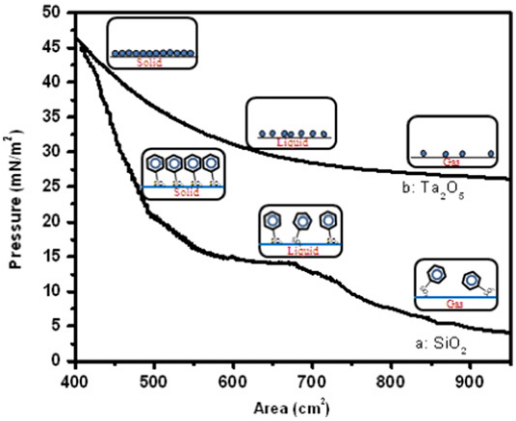


**Figure 1.** Pressure versus area isotherms of the Langmuir–Blodgett films of (a) phenyl-silica and (b) $Ta_2O_5$.

decreases from 950 $cm^2$ to 700 $cm^2$ which shows the widely spaced phenyl silica molecules have started coming closer to each other. Further decreasing area from 700 $cm^2$ to 570 $cm^2$ (second segment), the surface pressure remains almost constant. This part of the isotherm indicates the orientation of the phenyl silica molecules, possibly switches from edge-on to face-on and the phenyl rings start stacking with each other, thereby accommodating them in a smaller area (figure 1). In the third segment, the decrease in the area (from 570 $cm^2$ to 400 $cm^2$), results in sharp increase in surface pressure which confirms the molecules are tightly packed and a compact monolayer is formed. Withdrawal of the substrate was initiated at the surface pressure value of 35 mN $m^{-2}$, as from the isotherm, it is evident that at this particular pressure, a uniform mono-molecular layer of phenyl silica molecules is formed at the air–water interface (figure 1).

On the other hand, the isotherm for fabrication of $Ta_2O_5$ films using LB film technique consists of two major segments (figure 1(b)). The first segment (950–650 $cm^2$) indicates that as the area is decreased, the surface pressure was gradually increased. In this segment of the isotherm, the widely spaced molecules were brought closer by the barriers. When the barriers were further compressed, a steep increase in the surface pressure (from 10 to 40 mN $m^{-2}$) was observed in the second segment of the isotherm, which signifies the formation of a close packed monolayer at the air–water interface. Withdrawal of the substrate was carried out at the surface pressure value of 25 mN $m^{-2}$. The dipping and lifting speed of the substrate was kept at 1 mm per minute. Once a monolayer was transferred from the air–water interface to the quartz substrate, it was allowed to dry at ambient condition for 20 min. After completion of film deposition, the films were heated at 650 °C in air for 6 h. Ph-$SiO_2$ and tantalum pentoxide film fabricated at room temperature were found to be amorphous in nature (figure S2). After annealing at 650 °C for 6 h in air, GAXRD patterns of the samples showed the presence of $Ta_2O_5$ which could be indexed in the orthorhombic crystal system with the space group Pmm2 (JCPDS no. 79-1375) as shown in figures 2(a) and (b). In figures 2(a) and (b) x-ray diffraction patterns correspond to the sample 10S–15T–10S–15T–10S–15T and 4S–6T–4S–6T respectively. Both show the presence of (010), (411), (1102) and (020) planes of $Ta_2O_5$. The normal $Ta_2O_5$–$SiO_2$ composite prepared by hydrothermal method was also found to be x-ray amorphous (figure S3). To improve the crystallinity of the product, heating of the product was carried out at 650 °C for 6 h in air and the PXRD pattern showed the presence of $Ta_2O_5$ (orthorhombic, space group Pmm2 (JCPDS no. 79-1375)) (figure 2(c)). TEM micrograph of the Langmuir film of phenyl silica deposited on the Cu grid (figure 3(a)) showed sheet-like structures. A low magnification TEM micrograph of the tantalum oxide (formed on the water surface due to the instantaneous hydrolysis of tantalum isopropoxide) also showed sheets with folded edges (figure 3(b)). A more careful observation indicates that the sheets were actually comprised of tiny $Ta_2O_5$ nanoparticles. The HRTEM image (inset of figure 3(b)) confirms the formation of $Ta_2O_5$ nanoparticles as the measured inter-planar distance corresponds to the (010) plane of $Ta_2O_5$. The TEM image of the bulk $SiO_2$–$Ta_2O_5$ composite powder (figure 3(c)) showed spherical particles of size around 70 nm with rough surfaces. TEM-EDX study confirms the presence of Si, Ta and O in the sample (figure S4). Weight percentages of oxygen, silicon and tantalum in the sample as obtained from the quantification of the EDX spectra were 1.00, 0.50 and 1.78% respectively.

From AFM studies, the thickness of monolayer silica LB film was found to be ~3 nm (figure 4(a)) and that of the monolayer $Ta_2O_5$ LB film is ~8 nm (figure 4(b)); whereas the thicknesses of the 10T and 6S–4T–6S–4T–6S films were found to be ~40 nm (figure S5(a)) and 139 nm respectively (figure S5(b)). AFM image of the 10S–15T–10S–15T–10S–15T sample (figure 4(c)) showed that the films are ~500 nm thick. FESEM imaging was carried out to study the surface morphology of the films. It was observed that the surface is rough (figure S6(a)).

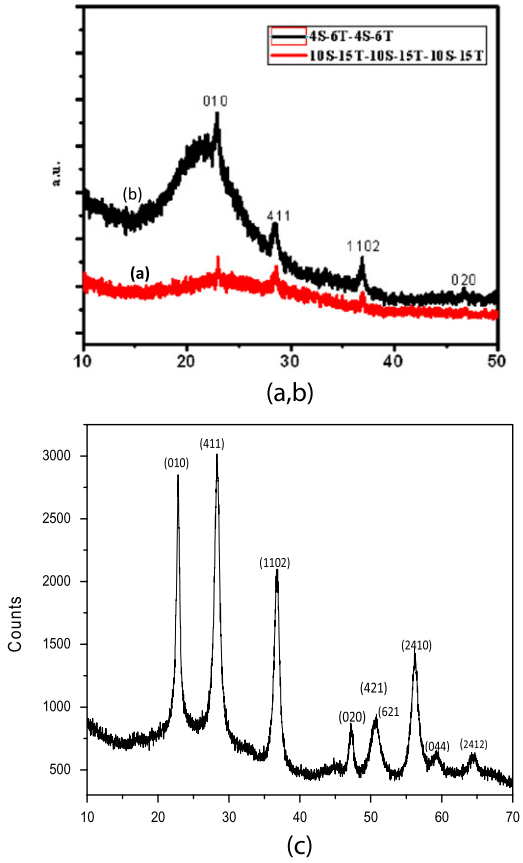


**Figure 2.** GAXRD patterns of annealed (a) 4S–6T–4S–6T and (b) 10S–15T–10S–15T–10S–15T (S: Silica and T: $Ta_2O_5$ monolayers); (c) PXRD pattern of $SiO_2$–$Ta_2O_5$ composite powder (after annealing).

Cross sectional FESEM image of the 10S–15T–10S–15T–10S–15T sample (figure S6(b)) was also recorded, so as to see the multilayered structure of the films. However, the boundary between two layers of silica or tantalum oxide could not be distinguished because of the high degree of diffusion of silica layer into tantalum pentoxide. The interlayer diffusion may be caused by the high temperature annealing.

When phenyl silica solution in chloroform is spread over the water sub-phase, it forms a self-assembled mono-molecular layer at the air–water interface. Besides its Lewis acidity, it can also act as a high surface area substrate for tantalum oxide. The BET surface area of the prepared silica particles was obtained (before forming their LB films), using nitrogen gas adsorption–desorption technique and found to be 162 $m^2\ g^{-1}$ (figure S7). BET analysis also suggests that the particles were mesoporous with average pore diameter of ~8 nm. Band gap values of the prepared $SiO_2$, $Ta_2O_5$ and $SiO_2/Ta_2O_5$ films obtained from DRS (figure 5) are shown in table 1. Band gap of bulk tantalum pentoxide is known to be 4.1 eV and that of silica is 8.9 eV. 4S–6T–4S–6T sample is found to have a band gap of 4.3 eV, whereas, band gap value rises to 4.6 in case of 6S–4T–6S–4T–6S. From the DRS spectra presented in figure 5, it is also evident that as the number of layers of silica and tantalum oxide increases, the concentration of the absorbing species is increased which in turn enhances the absorption maxima. Therefore in case of 10S–15T–10S–15T–10S–15T sample the absorption coefficient is three times higher than that of 4S–6T–4S–6T sample. It can be observed that with the increase in the amount of silica in the films, band gap has increased compared to that of bare $Ta_2O_5$. 10S–15T–10S–15T–10S–15T sample has the maximum band gap of 4.8 eV. Thus, we have shown the possibility of engineering of the optical properties like band gap by controlling the layer structures and this result is in close agreement with previous studies on nanostructure $SiO_2$–$Ta_2O_5$ composites [24].

### 4.2. Photocatalytic degradation of Rhodamine B

In order to study the photocatalytic dye degradation efficiency of the material, we have recorded the UV–visible absorption spectra of the dye solution at different time intervals. From the absorption maxima of the optical spectra, the relative concentration has been calculated at a particular point of time, as the absorption maxima for the initial concentration of the dye is known from the optical measurements. Since we have used quite low concentration of the dye, the spectra are assumed to follow the Beer–Lambert's law. Figure 6(a) shows the plot of

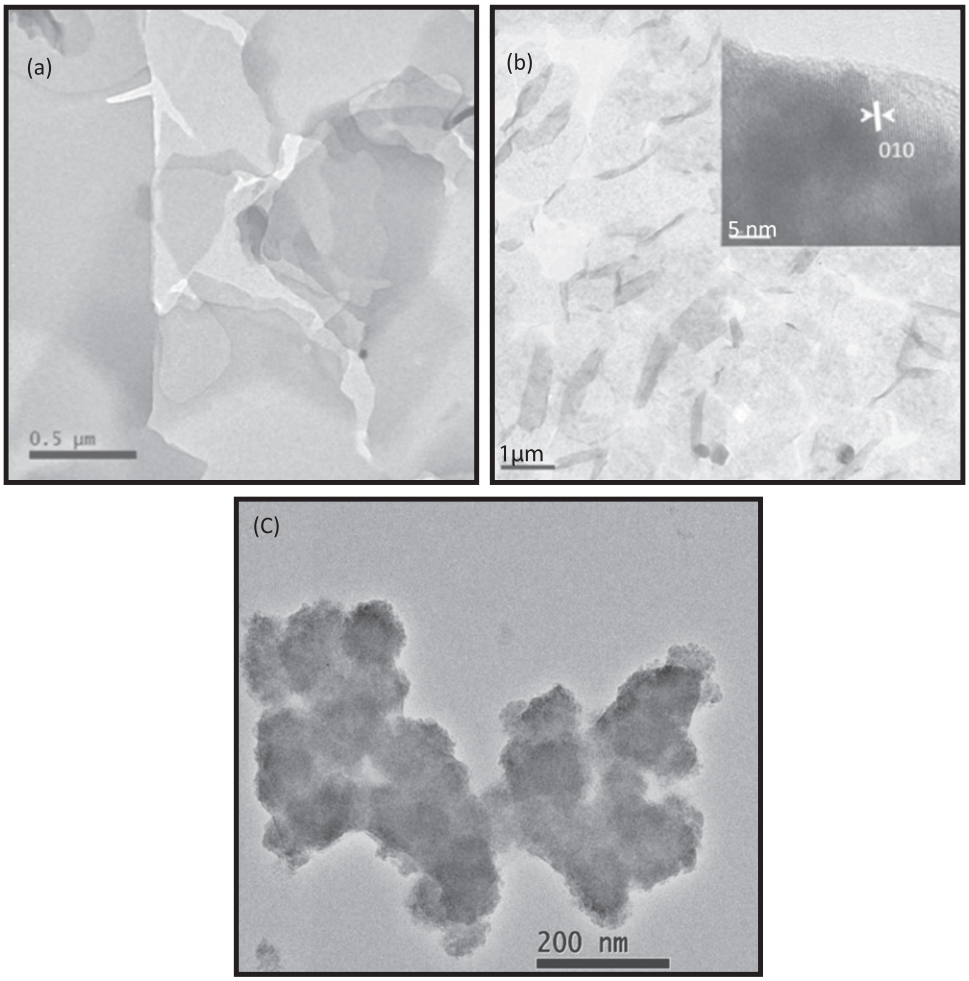


**Figure 3.** TEM images of the Langmuir film of (a) phenyl silica deposited on the Cu grid. (b) Tantalum oxide deposited on the Cu grid. (c) $SiO_2$–$Ta_2O_5$ composite powder (after annealing).

relative dye concentration ($C/C_o$) against irradiation time. The optimum photocatalytic activity of 10S–15T–10S–15T–10S–15T (per mg of the photocatalyst) was found to be 3.5 times higher than powdered silica–$Ta_2O_5$ composite. The photocatalytic degradation efficiency of the prepared films was summarized in the table 2. It can be observed that 10 layered LB film of pure tantalum oxide (10T) has poor degradation efficiency (22%). Although the sample 10T has the best efficiency of degradation per mg of the catalyst, its overall degradation efficiency and degradation per unit film area values are the lowest. For practical applications, overall degradation efficiency and degradation per unit film area values are more important than the efficiency of degradation per mg of the catalyst. However, 4S–6T–4S–6T and 10S–15T–10S–15T–10S–15T LB films have shown remarkable photocatalytic activity in the presence of tantalum oxide layer at the top of the multilayered film with higher concentration of $Ta_2O_5$ than silica. In case of 6S–4T–6S–4T–6SLB films, where silica is on the top, the photocatalytic activity is lower than that of 4S–6T–4S–6T and 10S–15T–10S–15T–10S–15TLB films. It is known that silica is not photoactive material; however, it helps in lowering e–h recombination, increasing absorption of dye and then transport to the photoactive site ($Ta_2O_5$ layer). The $Ta_2O_5$ layer being the only photoactive component of the films, needs to be exposed more towards irradiation which helps in enhancing the degradation of dyes.

In order to investigate the stability and reusability of the photocatalysts (LB films), the films were washed with deionized water and reused for the successive photocatalytic experimental runs. As shown in figure 6(b), after three experimental cycles of photodegradation of RhB, the photocatalytic activity of the prepared LB film system (10S–15T–10S–15T–10S–15T) is retained over 90%. The overall degradation efficiency after the first, second and third cycles were found to be 69%, 67% and 61% respectively. The observed lowering in the efficiency of the photocatalyst films might be due to the blocking of the active sites by adsorbed dye molecules which were not removed from the surface of the films even after washing.

Overall degradation percentage as well as percentage degradation per unit area of the catalyst film is found to be the highest for the 10S–15T–10S–15T–10S–15T sample.

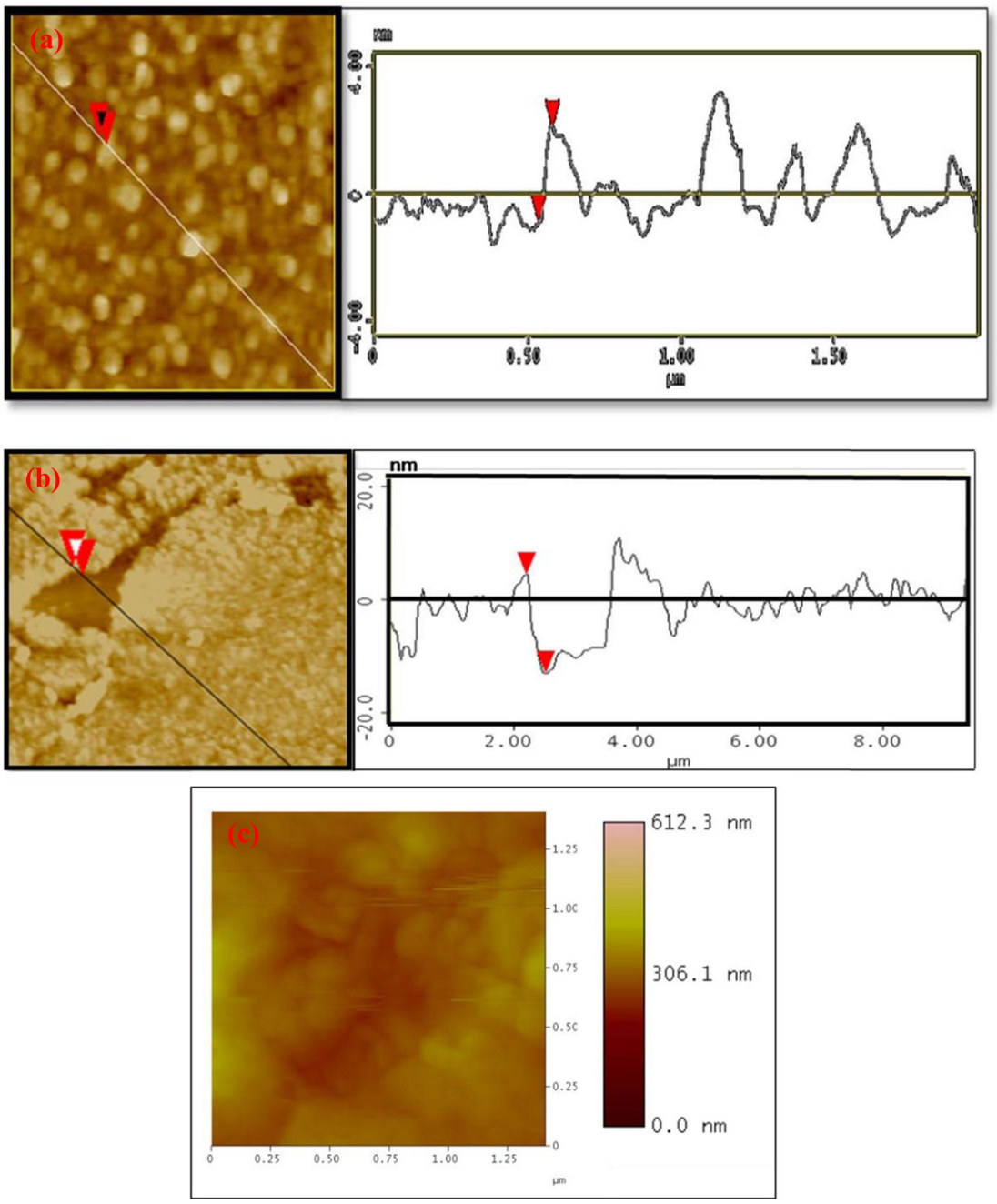


**Figure 4.** AFM images of (a) monolayer phenyl silica film; (b) monolayer of the $Ta_2O_5$ film, (c) 10S–15T–10S–15T–10S–15T films.

The experimental photocatalytic data were fitted to the pseudo first-order kinetic equation $\ln(Co/C) = -kt$ as shown in figure 7. It could be seen that the optimum rate of photocatalytic degradation using the 10S–15T–10S–15T–10S–15T sample is $8.91 \times 10^{-3}$ $min^{-1}$ which is five times higher than that of pure $Ta_2O_5$ and 1.5 times higher than the bulk composite powder. The superior photocatalytic property of the $SiO_2$–$Ta_2O_5$ complex films compared to the 10 layered film of pure tantalum oxide is due to the electron withdrawing nature of the silica, which shifts the conduction band of $Ta_2O_5$ to more negative values and its valence band to more positive values. Consequently, the recombination process for the excitons is delayed and hence, the process of photodegradation of organic dye is enhanced.

The effective separation of charge carriers is essential to improve photocatalytic efficiency [25]. Furthermore, photocatalytic efficiency is also affected by the surface area and dispersibility of the photocatalysts [26]. The enhanced contact area of LB films can provide efficient charge transfer and shorten the charge transport time and distance, thereby promoting the separation of electron–hole pairs. Under UV light irradiation, the electrons of $Ta_2O_5$ can be promoted to the conduction band, leaving holes in the valence band. In addition, the photocatalysts have functionalized $SiO_2$ which can trap the photo-induced electrons.

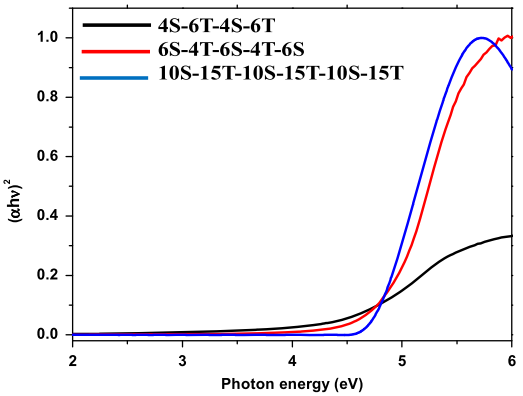


**Figure 5.** UV–Vis Diffuse Reflectance Spectra of the silica and $Ta_2O_5$ films.

**Table 1.** Band gap values of the LB films

| Sample name | Band gap (eV) (error: 0.1 eV) |
|---|---|
| Pure $Ta_2O_5$ | 4.1 |
| 4S–6T–4S–6T | 4.3 |
| 6S–4T–6S–4T–6S | 4.6 |
| 10S–15T–10S–15T–10S–15T | 4.8 |
| Pure silica | 8.9 |

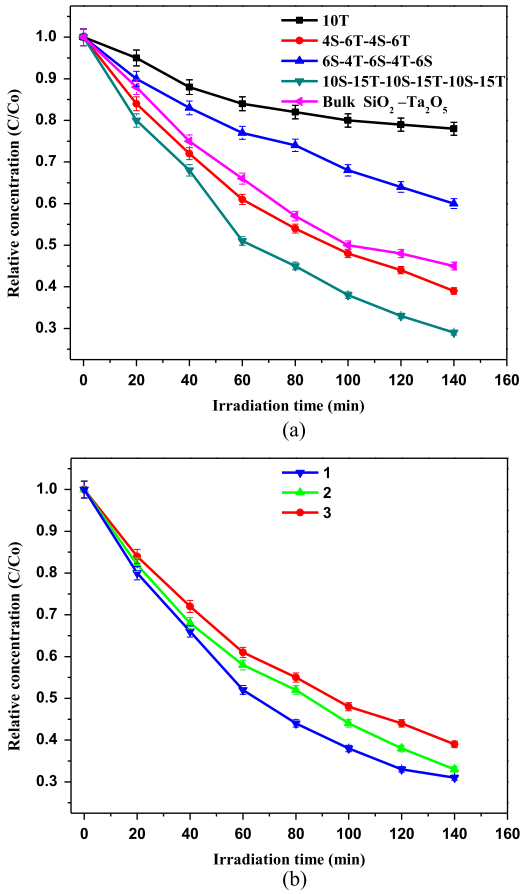


**Figure 6.** (a)The plot of relative concentration ($C/C_o$) versus irradiation time for the degradation of dye over LB film photocatalysts under UV light; (b) Recyclability study of the silica and tantalum pentoxide film (10S–15T–10S–15T–10S–15T) for three consecutive cycles.

**Table 2.** The photocatalytic efficiency of the prepared films expressed in terms of overall degradation percentage, degradation percentage per mg of the catalyst and the percentage degradation per unit area of the film

| Sample name | Overall degradation (%) | Degradation per mg of the catalyst: (%) | Degradation per unit area of the catalyst film: (%) (Film area = 3.75 $cm^2$) |
|---|---|---|---|
| 10T | 22 | 2.2 | 5.8 |
| 4S–6T–4S–6T | 61 | 1.3 | 16.2 |
| 6S–4T–6S–4T–6S | 40 | 0.9 | 10.6 |
| 10S–15T–10S–15T–10S–15T | 71 | 0.7 | 18.6 |
| Bulk $SiO_2$–$Ta_2O_5$ | 55 | 0.2 | |

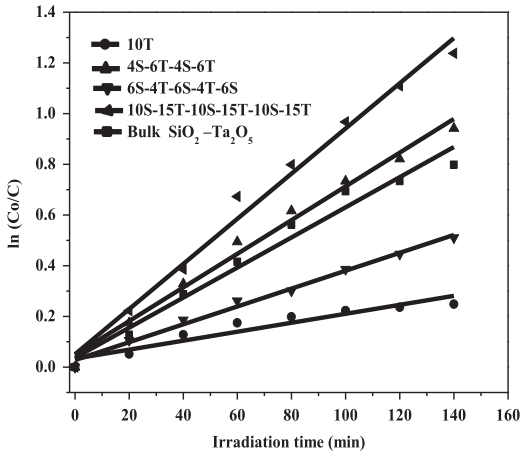


**Figure 7.** The plot of ln ($C_o/C$) versus irradiation time for the degradation of dye over LB film photocatalysts under UV light.

Subsequently, photo-induced electrons on $SiO_2$ surface can react with adsorbed $O_2$ in water to produce superoxide radical anion ($O_2^-$). Meanwhile, photoinduced holes can also readily react with surface bound hydroxyl anions to produce $^\bullet$OH. Thus, $^\bullet$OH and $O_2^-$ could result in the oxidative decomposition of the dye molecules in water.

### 4.3. Detection of reactive species

The enhanced photocatalytic performance of the as-prepared LB films motivated us to further investigate the pathway of the photocatalytic degradation process. Generally, photo-generated reactive species, mainly, trapped holes and $^\bullet$OH are expected to be involved in the photocatalytic process. To examine the role of these reactive species, the effect of radical scavengers on the photodegradation of RhB was investigated to propose the reaction pathway. Prior to UV-irradiation, different scavengers, viz, 10 vol % of t-butyl alcohol (TBA), 0.01 M of ammonium oxalate (AO) and 10 vol% of benzoquinone (BQ) were added into the RhB solution containing the 10S–15T–10S–15T–10S–15T sample. As can be seen from figure 8, a significant change was observed in the photocatalytic degradation of RhB by the addition of TBA as the $^\bullet$OH scavenger compared with reactions with no scavenger under same experimental conditions. Addition of BQ as super oxide radical scavenger does not show any considerable reduction in the process of photodegradation; which implies that super oxide radical anions are not the major reactive species. However, the degradation rate is drastically inhibited by the addition of AO as hole scavenger, indicating that the trapped holes are the main active oxidative species of the LB film photocatalyst.

Photocurrent measurements were done on an electrochemical workstation (ZAHNER IM6e Electrik, Germany) based on a conventional three-electrode system comprised of indium–tin oxide coated with photocatalyst as the working electrode, platinum wire as the counter electrode, and Ag/AgCl (3 N KCl) as the reference electrode. The transient photocurrent responses of the pure $Ta_2O_5$ sample and LB film photocatalyst were examined for several on–off cycles of irradiation by UV light, in order to give further evidence to support the proposed photocatalytic mechanism. 0.01 M $Na_2SO_4$ aqueous solution was used as the electrolyte. It can be clearly seen from figure 9, that for the bare $Ta_2O_5$ sample, the photocurrent density was found to be only 0.1 mA $cm^2$, whereas, for the LB film sample (10S–15T–10S–15T–10S–15T), the photocurrent density value goes upto 0.36 mA.$cm^2$. The LB film photocatalyst exhibited remarkable photocurrent responses which is 3.6

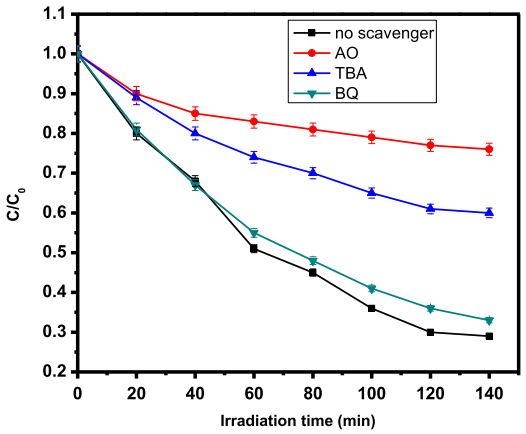


**Figure 8.** Effect of different scavengers on the degradation of RhB (for the 10S–15T–10S–15T–10S–15T sample) under UV light.

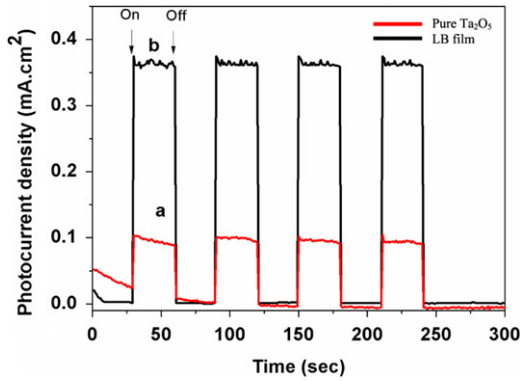


**Figure 9.** The transient photocurrent response of the pure $Ta_2O_5$ and LB film (10S–15T–10S–15T–10S–15T) photocatalysts for 4 ON–OFF cycles.

times higher than pure $Ta_2O_5$ under UV light irradiation for four on–off cycles. The photoelectrochemical results indicate the better separation efficiency of photo generated electron–hole pairs at the interface of the $SiO_2$ and $Ta_2O_5$ heterostructured system. Therefore, the photocurrent results confirm the discussion on the charge carrier separation for improved photocatalytic performance.

## 5. Conclusions

We have successfully deposited several layers of $SiO_2$ and $Ta_2O_5$ (alternating) on quartz substrate by LB technique. Interestingly, these complex multilayered films exhibited enhanced photocatalytic activity in the degradation of Rhodamine B. The activity of the LB films is highly dependent on the area of contact between the $SiO_2$ and $Ta_2O_5$ in the film, which was enhanced by the layer by layer self-assembly of silica and tantalum oxide. The photocatalytic activity of these films was also sensitive to the sequence of silica and tantalum oxide layers when the film area of all the samples was kept constant (3.75 $cm^2$) with the tantalum oxide terminated multilayers showing higher photocatalytic efficiency. The optimum photocatalytic activity of the LB film (10S–15T–10S–15T–10S–15T) was much higher than the bulk composite powder. The enhanced photocatalytic performance of the LB films is due to synergistic effect including the high separation efficiency of photo-generated electron-hole pair and the higher contact area between tantalum oxide and silica layers.

Electronic Supplementary Information (ESI) available on the WWW under stacks.iop.org/MRX/2/056404/mmedia. It contains the list of figures including the TEM image of the phenyl-silica nanoparticles, GAXRD patterns of 10S–15T–10S–15T–10S–15T LB films and silica–tantalum oxide bulk composite before heating; the cross-sectional FESEM images of 10S–15T–10S–15T–10S–15T LB films and BET nitrogen gas adsorption desorption isotherm for the silica (powdered) samples.

## Acknowledgment

AKG thanks Department of Science and Technology (Nanomission), Department of Electronics and Information Technology (Deity) Govt. of India for financial support. AB thanks UGC for fellowship.

## References

[1] Asahi R, Morikawa T, Ohwaki T, Aoki K and Taga Y 2001 *Science* **293** 269–71
[2] McFarland E W and Tang J 2003 *Nature* **421** 616–8
[3] Gordon R G, Becker J, Hausmann D and Suh S 2001 *Chem. Mater.* **13** 2463–4
[4] Ming W, Bi C, Li L, Long S, Liu Q, Lu H, Lu N, Sun P and Liu M 2014 *Nat. Commun.* **5** 1–6
[5] Nie X, Leyland A, Song H W, Yerokhin A L, Dowey S J and Matthews A 1999 *Surf. Coat. Technol.* **116** 1055–60
[6] Antipina M N, Bykov I V, Gainutdinov R V, Koksharov Y A, Malakho A P, Polyakov S N, Tolstikhin A L, Yurov T V and Khomutov G B 2002 *Mater. Sci. Eng.* C **22** 171–6
[7] Chi L F, Rakers S, Hartig M, Fuchs H and Schmid G 1998 *Thin Solid Films* **327** 520–3
[8] Sawunyama P, Fujishima A and Hashimoto K 1999 *Langmuir* **15** 3551–6
[9] Zhang C R, Yang K J and Jin W R 1996 *Thin Solid Films* **284** 533–6
[10] Hussain S A and Bhattacharjee D 2009 *Mod. Phys. Lett.* B **23** 3437–51
[11] Takahara Y, Kondo J N, Takata T, Lu D and Domen K 2001 *Chem. Mater.* **13** 1194–9
[12] Yu N, Lee B, Domen K and Kondo J N 2008 *Chem. Mater.* **20** 5361–7
[13] Sharma M, Das D, Baruah A, Jain A and Ganguli A K 2014 *Langmuir* **30** 3199–208
[14] Hideki K, Asakura K and Kudo A 2003 *J. Am. Chem. Soc.* **125** 3082–9
[15] Oosawa Y and Gratzel M 1988 *J. Chem. Soc. Faraday Trans.* I **84** 197–205
[16] Xin Z, Zhang F and Chan K Y 2005 *Appl. Catalysis A: Gen.* **284** 193–8
[17] Bayati M R, Alipour H M, Joshi S, Molaei R, Narayan R J, Narayan J and Misture S T 2013 *J. Phys. Chem.* C **117** 7138–47
[18] Hyeok C, Stathatos E and Dionysiou D 2006 *Appl. Catalysis B: Environ.* **63** 60–7
[19] Yasutaka T and Matsuoka Y 1988 *J. Mater. Sci.* **23** 2259–66
[20] Das N M, Roy D and Gupta P S 2013 *Mater. Res. Bull.* **48** 4223–9
[21] Schurr M, Seidl M, Brugger A and Voit H 1999 *Thin Solid Films* **342** 266–9
[22] Shortell M P, Liu H W, Zhu H, Jaatinen E A and Waclawik E R 2010 *Langmuir* **26** 14472–8
[23] Stöber W and Fink A 1968 *J. Colloid Interface Sci.* **26** 62–9
[24] Ndiege N, Chandrasekharan R, Radadia A D, Harris W, Mintz E, Masel R I and Shannon M A 2011 *Chem. Eur. J.* **17** 7685–93
[25] Kudo A and Miseki Y 2009 *Chem. Soc. Rev.* **38** 253–78
[26] Takanabe K and Domen K 2011 *Green* **1** 313–22